

This manuscript is a preprint and has been submitted for publication in GEOLOGY. Please note that subsequent versions of this manuscript may have different content.

If accepted, the final version of this manuscript will be available via the 'Peer reviewed Publication DOI' link on the right hand side of this webpage.

Please feel free to contact any of the authors, we welcome feedback!

Inclination and heterogeneity of layered geological sequences influence dike-induced ground deformation

Matías Clunes¹, John Browning^{1,2,3}, Carlos Marquardt^{1,3}, Jorge Cortez¹, Kyriaki Drymoni⁴, and Janine Kavanagh⁵

¹Department of Structural and Geotechnical Engineering, Pontificia Universidad Católica de Chile, Santiago, Chile

²Andean Geothermal Centre of Excellence (CEGA), Universidad de Chile, Santiago, Chile

³Department of Mining Engineering, Pontificia Universidad Católica de Chile, Santiago, Chile

⁴Department of Earth and Environmental Sciences, Università degli Studi di Milano-Bicocca, Milan, Italy

⁵School of Environmental Sciences, University of Liverpool, Liverpool, United Kingdom

ABSTRACT

Constraints on the amount and pattern of ground deformation induced by dike emplacement are important for assessing potential eruptions. The vast majority of ground deformation inversions made for volcano monitoring during volcanic unrest assume that dikes are emplaced in either an elastic-half space (a homogeneous crust) or a crust made of horizontal layers with different mechanical properties. Here, we extend these models by designing a novel set of two-dimensional Finite Element Method numerical simulations that consider dike-induced surface deformations related to a mechanically heterogeneous crust with inclined layers, thus modelling a common geometry in stratovolcanoes and crustal segments that have been folded by tectonic forces. Our results confirm that layer inclination can produce localized ground deformations which may be up to 40 times higher in terms of

deformation magnitude than would be expected in a non-layered model, depending on the angle of inclination and the stiffness of the rock units that host, and are adjacent to the dike. Generated asymmetrical deformation patterns produce deformation peaks located as much as 1.4 km away from those expected in non-layered models. These results highlight the necessity to accurately quantify both the mechanical properties and attitude of the geology underlying active volcanoes.

Keywords: Magmatic intrusion, inclined layers, surface deformation, volcano deformation, volcano heterogeneity

INTRODUCTION

Volcanic eruptions can occur when a magma-filled fracture (a dike, sill or inclined sheet) propagates from a magma source through the crust to the surface (Gudmundsson et al., 1999; Rivalta et al., 2015, Acocella, 2021). Magma emplacement deforms the crust resulting in surface uplift or subsidence signals that can be measured and used to infer information about intrusion depth, volume, shape and orientation, and which may be useful for determining potential eruption characteristics (Geshi et al., 2020). However, the vast majority of models used in volcano monitoring to infer the deformation associated with magmatic emplacement assume that the crust is either isotropic (an elastic half-space) (e.g., Okada, 1985; Mantiloni et al., 2020), or mechanically stratified with horizontal layers (Masterlark, 2007; Bazargan and Gudmundsson, 2019; 2020). Both assumptions are likely simplifications, especially in areas where volcanoes are built atop highly folded and deformed rocks, such as in Cordillera settings (Clunes et al., 2021). In addition to inclined layers underlying a volcano, that may dip either outwards or inwards towards the volcano center, the slopes of the upper parts of many stratovolcanoes are inclined by as much as 42° (Gudmundsson, 2012; Grosse et al., 2014;). In both of these situations it is not reasonable to always assume that dikes propagate

through solely horizontal layers. It is also now well known that rock layers that constitute a volcano may vary considerably in terms of their mechanical properties (Drymoni et al., 2020; Heap et al., 2020; Kendrick et al., 2021; Maccaferri et al., 2010). Given these observations, it is perhaps likely that most dikes are emplaced in heterogeneous crustal segments with layers that are somewhat inclined, even in extensional settings albeit the layer inclination may be minor or close to horizontal near the surface (e.g., Gudmundsson, 1983). Therefore, it is necessary to constrain the deformation signals associated with both heterogeneous and inclined layered sequences and compare the differences associated with commonly used simplified crustal assumptions. There have been attempts to constrain the crustal stress field (e.g., Gudmundsson, 2006) and deformation (e.g., Manconi et al., 2007; and Masterlark, 2007) associated with magma chamber inflation using either a simple dipping sequence in Iceland (Gudmundsson, 2006) or horizontal heterogeneous layered sequences (Masterlark, 2007). Masterlark (2007) demonstrated using a combination of analytical and finite element models that the widely used Mogi (1958) model, which considers a point-pressure source embedded in a homogeneous, isotropic segment, can generate substantial displacement prediction errors and significantly inaccurate deformation source parameters if the crustal unit is heterogeneous. In that work, the presence of weak layers in a caldera resulted in a deformation source located more than 1 km deeper compared to the source depth obtained using the elastic half-space assumption. Bazargan and Gudmundsson (2019; 2020), analyzed both the stresses and displacements generated at the surface by dikes and inclined sheets intruding horizontally layered rocks. They showed that the presence of compliant layers (with low Young's modulus) increases the surface deformation expressed during dike or inclined sheet emplacement, and that intrusions meeting layered sequences at lower angles generates larger surface displacements. Although significant progress has been made in volcano

monitoring in the past decades (Gudmundsson et al., 2022) we still cannot yet forecast with any certainty when and where a magmatic dike will emplace or erupt. This becomes further complicated in highly deformed crustal settings such as the Andes where the host rock is commonly formed by rock layers inclined at different angles, in part because understanding of the role of crustal properties and geometry through which the dikes propagate is lacking. Here we present a series of novel 2D numerical models using the Finite Element Method (FEM) that consider dike-induced ground deformation resulting from a crustal segment hosting contrasting mechanical properties and with variably dipping layers.

NUMERICAL MODEL SETUP

The FEM software COMSOL Multiphysics 5.4 was used to analyze dike-induced surface displacements in a layered crustal segment comprising either horizontal or inclined layers (Figures 1A and 1B). The dimensions of the layered crustal segment hosting the dike were 20 km wide x 20 km deep, tested as being sufficient to avoid boundary effects (Supplemental Material Figures S1-S2). The dike was modeled as an elliptical cavity of 1 m thickness and its geometry and location in the model domain was varied by changing both the dike length and emplacement depth between 1, 2 and 4 km. The crustal segment hosting the dike was modeled as a linear-elastic solid since the primary interest was on the influence of elastic properties on ground deformation. The inclined layers, with contrasting elastic properties (Young's modulus ratios), were made to dip by 10, 25 and 45°. Both the upper and lower layers were assigned alternating Young's modulus of either 1, 10 or 100 GPa such that four stiffness ratios were examined between the different models, 100:1, 10:1, 1:10, 1:100, where the first number relates to the layer hosting the dike (E_1) and the second to the layer above the dike (E_2). These stiffness values were chosen to encompass a wide range of rocks, such as compliant pyroclastic rocks and stiff lava flows (Gudmundsson, 2011). To compare our

results with the more common modeling protocol we also tested a horizontally layered sequence using the aforementioned contrasting elastic properties and a non-layered crustal segment with only one Young's modulus of 50 GPa. The only boundary load in the model comes from an internal magmatic overpressure (P_0) of 5 MPa. The upper boundary of the model is a free surface, and it is along this surface that the horizontal and vertical displacements were measured. The other boundaries of the model are fixed, indicated by crosses, so as to avoid rigid-body translation and rotation. The dipping layers are always located in the right-side of the crustal segment starting at the center of the domain, above the dike tip. More information about the modeling setup is provided in the Supplementary Material.

VERTICAL GROUND DISPLACEMENTS

Figure 2 presents profiles of vertical displacement along the upper free surface induced by a 2 km high dike with its upper tip emplaced at 2 km depth. Results from other dikes modeled are provided in the Supplementary Material Figures S4-S19. In both the non-layered and horizontally layered models, the vertical ground displacement is symmetrically distributed and peaks between around 2.4 km and 4.8 km on either side of the dike (Figure 2). The vertical ground displacement becomes asymmetrically distributed when the inclined layers are modeled, and the magnitude of vertical deformation becomes greater with lower Young's modulus ratios (Figures 2B and 2D).

When the layer hosting the dike is stiffer than the inclined layer, the vertical displacements are greatest in the layer hosting the dike (Figures 2A and 2C). Conversely, when the layer hosting the dike is more compliant than the upper layer, the vertical displacement is greatest in the layer hosting the dike (Figures 2B and 2D). In this case, when the inclined layer is stiff, the asymmetric deformation is more pronounced when the stiffness contrast is greatest (i.e.,

1:100 rather than 1:10). In this case the maximum peak of vertical displacement is located up to 1.4 km (in the 45° model) away from the dike than compared with the homogeneous model. However, the opposite is found when the inclined layer is compliant such that the larger stiffness contrast (100:1) demonstrates a more symmetrical deformation pattern than the lower stiffness contrast (10:1). When the upper layer is compliant, the amount of vertical ground displacement increases with layer inclination. For example, in the 10:1 case (Figure 2C) for the upper layer dipping at 45° the maximum vertical displacement is 19 cm, at 25° is 16.3 cm, and at 10° is 13.5 cm. The opposite pattern is observed when the upper layer is stiff, such that the amount of vertical surface displacement decreases with layer inclination. For example, in the 1:10 case with the layer dipping at 10° the maximum vertical displacement is 83 cm, at 25° is 51 cm and at 45° is 29 cm (Figure 2D).

HORIZONTAL GROUND DISPLACEMENTS

Figure 3 reports horizontal displacement along the upper free surface of the model domain for the Young's modulus ratios tested where the position of the center of the dike is again marked at zero. In both the non-layered and horizontally layered models the horizontal ground displacement is symmetrically distributed and peaks between 4.4 km and 7 km on either side of the dike. In these results, the component of horizontal displacement is oriented with respect to the center of displacement above the dike, such that negative horizontal displacement simply represents ground movement in the opposite direction with respect to the positive values. In all cases the overall deformation signal is extensional, such that each side of the model domain above the dike move away from one another, as expected during dike emplacement. However, when the modeled layers are inclined, the amount of horizontal displacement is different above the area with the inclined layer than the area without the layer and so the extension is asymmetric. This effect is most pronounced when the inclined layer

is stiffer than the layer hosting the dike (Figure 3B and 3D). In this case the maximum peak offset is located 2.4 km away compared to the horizontally layered model for an inclination of 10° and 1.1 km away from the homogeneous model for an inclination of 45° . When the inclined layer is compliant (Figures 3A and 3C), the amount of horizontal ground displacement recorded over the inclined layer increases with layer inclination. For example, in the 10:1 case (Figure 3C) with the layer dipping at 45° the maximum horizontal displacement is 29.1 cm, at 25° is 25.1 cm and at 10° is 19.9 cm. As observed for vertical ground deformation, the amount of horizontal surface deformation recorded over the inclined layer decreases with layer inclination when the layer above the dike is stiff. This effect is more pronounced when the stiffness ratio is 1:10 as observed in Figure 3D. In this case the maximum horizontal deformation with the layer dipping at 10° is 42.2 cm, at 25° is 34.6 cm and at 45° is 25.6 cm.

DISCUSSION AND CONCLUSION

The results indicate that for any study attempting to invert ground deformation measurements to determine dike emplacement processes, it is necessary to constrain, as best as possible, both the mechanical properties of the geological units and their attitudes, especially the amount by which the layers dip. Figure 4 shows the change in vertical and horizontal ground deformation with respect to the non-layered cases recorded for each tested stiffness ratio and layer inclination. The comparison highlights that layer inclination, in the stiff to compliant setup (high E_1 , low E_2), is a principal contributor to increasing surface deformation, while in the compliant to stiff setup (low E_1 , high E_2) is a principal contributor to decreasing surface displacement. A series of model fits describe the relationship between changes in ground displacement, layer inclination and stiffness ratios. We suggest that when the geology of a volcanic zone is well-characterized in terms of the rock mechanical properties and attitudes,

it should be possible to derive a similar series of curves so as to be able to estimate the contribution of the component of ground deformation associated specifically with the layered sequence amplification effect reported.

Our numerical results can be explained by considering the area of the different modeled rock layers which in nature are represented as rock volumes. The angle at which each individual unit dips will alter the amount of deformable available material since the area of the upper layer changes depending on the angle of inclination (Figure 4C). The displacement amount increases or decreases because the area of the stiff layer reduces or increases with respect to the area of the compliant layer. As we show in our results, the larger the area of the stiff unit, the less the deformation and vice versa, and in these simplistic models it is the angle of inclination of the contact between the units which controls the area. It is then expected, and quantifiable, that the area over which compliant or stiff rocks are located will deform more or less as a function of both the rocks Young's modulus and area. In nature, the calculation of layer areas would likely be more complex and involve multiple layers, but the physical processes described here remain. Further work should aim to fully characterize both the mechanical properties and layer geometries of crustal zones hosting volcanoes in order to delineate their relative influence on recorded surface displacements.

Our models have shown that the combination of mechanical heterogeneity (e.g., Masterlark, 2007) and layer inclination can substantially alter dike-induced ground deformation signals which can become highly asymmetric and as much as 40 times different than if assuming a homogeneous elastic half-space model. The asymmetric ground deformation profiles demonstrated are similar to those generated in other numerical and analogue models of inclined sheet emplacement (e.g., Kavanagh et al., 2018; Bazargan and Gudmundsson, 2020). This suggests that it is equally important to consider the geometry of the rock units into which

a magmatic intrusion emplaces as well as the intrusion geometry because similar deformation signals could be generated by vertical or inclined intrusions depending on the presence of inclined and stratified layered sequence. Whilst in our models the ground surface is flat, further complexities may arrive when introducing both topography (e.g., Trasatti et al., 2003; Johnson et al., 2019) with layer inclination and so this should be further investigated. Other studies (e.g., Magee et al., 2017, Poppe et al., 2019) have shown that deformation can be partly accommodated by fractures surrounding magmatic intrusions which also influence surface deformation signals. We do not consider such dislocations or inelastic deformations but combined with the data presented here further highlight the need to accurately characterize crustal structure to correctly determine intrusive processes. Furthermore, Masterlark (2007) suggests that differences in Poisson's ratio between layers can alter deformation signals by as much as 40% and so combining such properties into inclined layer models may also be of value. Ultimately, to test such models, more must be known about the stratigraphy underlying volcanoes and the variation in mechanical properties of the geological units (e.g., Kendrick et al., 2021). Our models could be tested using analogue techniques (e.g., Kavanagh et al., 2018) and a dedicated volcano deformation study combining these data with ground displacement measurements is paramount.

ACKNOWLEDGEMENTS

We wish to thank the Editor William Clyde, as well as Agust Gudmundsson, Craig Magee and an anonymous reviewer for comments that helped improve the manuscript. This research was supported by ANID, through FONDECYT projects 11190143 and 1210591 and by the Clover 2030 Open-Seed Fund. MC acknowledges support from ANID 21202065. JK acknowledges a UKRI Future Leaders Fellowship MR/S035141/1. All models and data can

be accessed from DOI: (pending from PMDMeta repository), and are given in the supplemental material.

REFERENCES CITED

- Acocella, V, 2021, Volcano-tectonic Processes. *Advances in Volcanology*, Springer-Nature, Heidelberg, 537 p.
- Bazargan, M., and Gudmundsson, A., 2019. Dike-induced stresses and displacements in layered volcanic zones. *Journal of Volcanology and Geothermal Research*, 384, 189-205.
- Bazargan, M., and Gudmundsson, A., 2020, Stresses and displacements in layered rocks induced by inclined (cone) sheets. *Journal of Volcanology and Geothermal Research*, 401, 106965.
- Clunes, M., Browning, J., Cembrano, J., Marquardt, C., and Gudmundsson, A., 2021, Crustal folds alter local stress fields as demonstrated by magma sheet—Fold interactions in the Central Andes. *Earth and Planetary Science Letters*, 570, 117080.
- Drymoni, K., Browning, J., and Gudmundsson, A., 2020, Dyke-arrest scenarios in extensional regimes: Insights from field observations and numerical models, Santorini, Greece. *Journal of Volcanology and Geothermal Research*, 396, p.106854.
- Geshi, N., Browning, J., and Kusumoto, S., 2020, Magmatic overpressures, volatile exsolution and potential explosivity of fissure eruptions inferred via dike aspect ratios. *Scientific reports*, 10(1), 1-9.
- Grosse, P., Euillades, P.A., Euillades, L.D. and Van Wyk de Vries, B., 2014, A global database of composite volcano morphometry. *Bulletin of Volcanology*, 76(1), pp.1-16.

- Gudmundsson, A., 1983, Form and dimensions of dykes in eastern Iceland. *Tectonophysics*, 95(3-4), 295-307.
- Gudmundsson, A., Marinoni, L.B., and Marti, J., 1999, Injection and arrest of dykes: implications for volcanic hazards. *Journal of Volcanology and Geothermal Research*, 88(1-2), pp.1-13.
- Gudmundsson, A., 2002, Emplacement and arrest of sheets and dykes in central volcanoes. *Journal of Volcanology and Geothermal Research*, 116(3-4), 279-298.
- Gudmundsson, A., 2006, How local stresses control magma-chamber ruptures, dyke injections, and eruptions in composite volcanoes. *Earth-science reviews*, 79(1-2), pp.1-31.
- Gudmundsson, A., and Philipp, S. L., 2006, How local stress fields prevent volcanic eruptions. *Journal of Volcanology and Geothermal research*, 158(3-4), 257-268.
- Gudmundsson, A., 2011, *Rock fractures in geological processes*. Cambridge University Press. 578.
- Gudmundsson, A., 2012, Strengths and strain energies of volcanic edifices: implications for eruptions, collapse calderas, and landslides. *Natural Hazards and Earth System Sciences*, 12(7), 2241-2258.
- Gudmundsson, A., 2020, *Volcanotectonics: Understanding the Structure, Deformation and Dynamics of Volcanoes*. Cambridge: Cambridge University Press. doi:10.1017/9781139176217
- Johnson, J. H., Poland, M. P., Anderson, K. R., and Biggs, J., 2019. A cautionary tale of topography and tilt from Kilauea Caldera. *Geophysical Research Letters*, 46(8), 4221-4229.

- Kavanagh, J.L., Burns, A.J., Hazim, S.H., Wood, E.P., Martin, S.A., Hignett, S. and Dennis, D.J., 2018, Challenging dyke ascent models using novel laboratory experiments: Implications for reinterpreting evidence of magma ascent and volcanism. *Journal of Volcanology and Geothermal Research*, 354, pp.87-101.
- Kendrick, J.E., Schaefer, L.N., Schaubroth, J., Bell, A.F., Lamb, O.D., Lamur, A., Miwa, T., Coats, R., Lavallée, Y. and Kennedy, B.M., 2021, Physical and mechanical rock properties of a heterogeneous volcano: the case of Mount Unzen, Japan. *Solid Earth*, 12(3), pp.633-664.
- Maccaferri, F., Bonafede, M. and Rivalta, E., 2010, A numerical model of dyke propagation in layered elastic media. *Geophysical Journal International*, 180(3), pp.1107-1123.
- Magee, C., Bastow, I.D., van Wyk de Vries, B., Jackson, C.A.L., Hetherington, R., Hagos, M., and Hoggett, M., 2017, Structure and dynamics of surface uplift induced by incremental sill emplacement. *Geology*, 45(5), 431-434.
- Mantiloni, L., Nespoli, M., Belardinelli, M. E., & Bonafede, M., 2020, Deformation and stress in hydrothermal regions: The case of a disk-shaped inclusion in a half-space. *Journal of Volcanology and Geothermal Research*, 403, 107011.
- Masterlark, T., 2007, Magma intrusion and deformation predictions: Sensitivities to the Mogi assumptions. *Journal of Geophysical Research: Solid Earth*, 112(B6).
- Mogi, K., 1958, Relations between the eruptions of various volcanoes and the deformations of the ground surface around them, *Bull. Earthquake Res. Inst. Univ. Tokyo*, 36, 99–134.
- Okada, Y., 1985, Surface deformation due to shear and tensile faults in a half-space. *Bulletin of the seismological society of America*, 75(4), 1135-1154.

Poppe, S., Holohan, E. P., Galland, O., Buls, N., Van Gompel, G., Keelson, B., Tournigand, P., Brancart, J., Hollis, D., Nila, A., and Kervyn, M., 2019, An inside perspective on magma intrusion: Quantifying 3D displacement and strain in laboratory experiments by dynamic X-ray computed tomography. *Frontiers in Earth Science*, 7, 62.

Rivalta, E., Taisne, B., Bungler, A.P. and Katz, R.F., 2015, A review of mechanical models of dike propagation: Schools of thought, results and future directions. *Tectonophysics*, 638, pp.1-42.

Trasatti, E., Giunchi, C., and Bonafede, M., 2003, Effects of topography and rheological layering on ground deformation in volcanic regions. *Journal of Volcanology and Geothermal Research*, 122(1-2), 89-110.

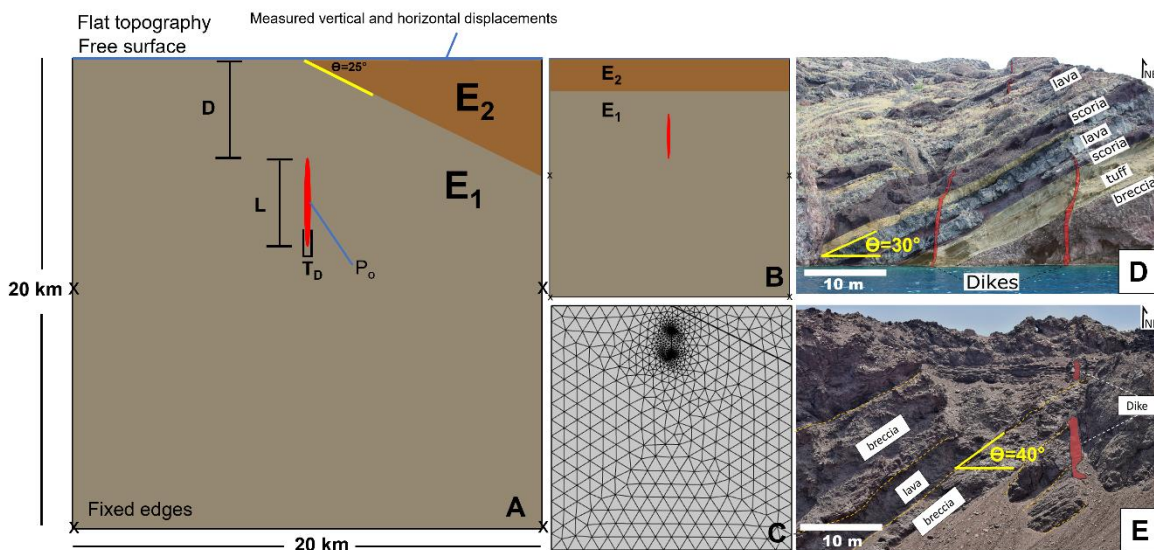


Figure 1: A) FEM model setup for the various layer inclinations tested (L : dike length, T_D : dike thickness, D : upper dike tip depth, P_o : magmatic overpressure, θ : layer inclination, E_1 - E_2 : alternating Young's modulus). B) Horizontally mechanical layered model setup C) Example of the model mesh with layers inclined at 25° . D) and E) Field photographs of dikes emplaced in dipping rock units from Santorini volcano (Greece) and the Andes (Chile),

respectively. The location of both case studies is provided in the Supplementary Material

Figure S3. B) and C) are not to scale.

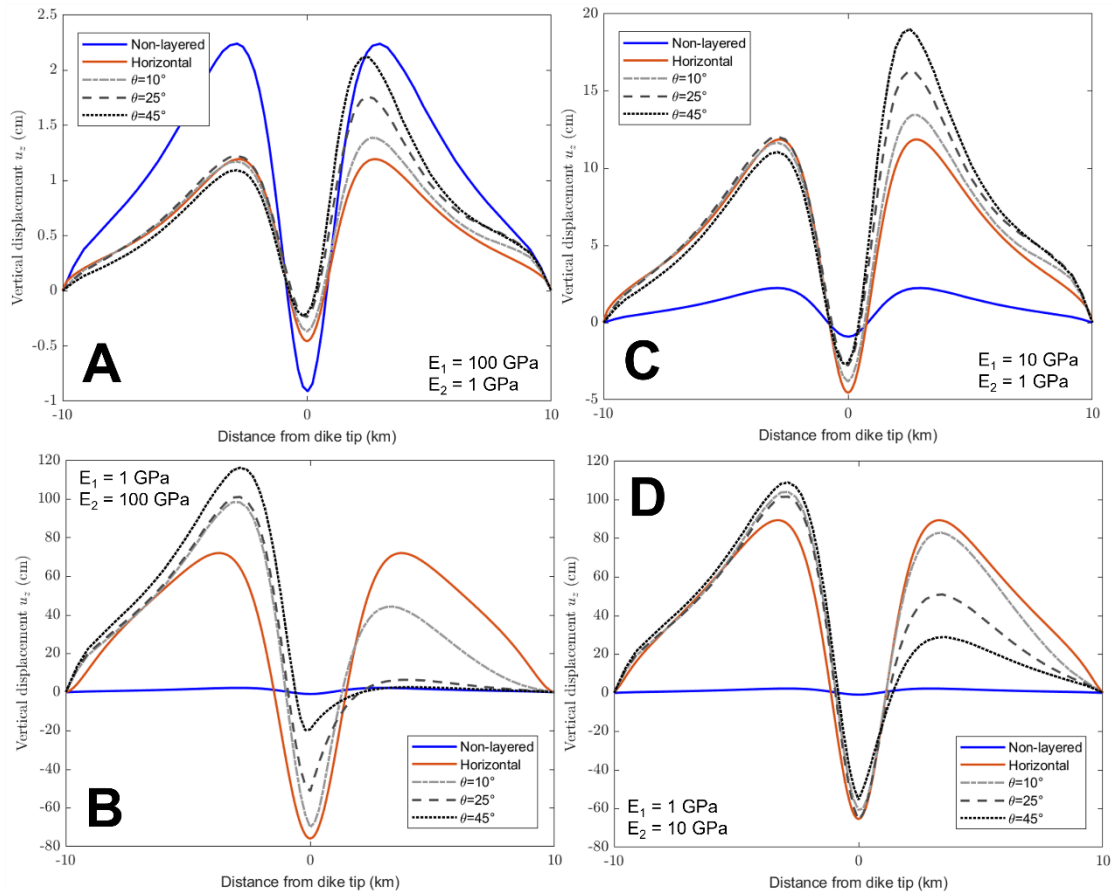


Figure 2: Vertical ground displacement (u_z) variations relative to the lateral distance from the dike tip for each layer inclination and stiffness contrast tested.

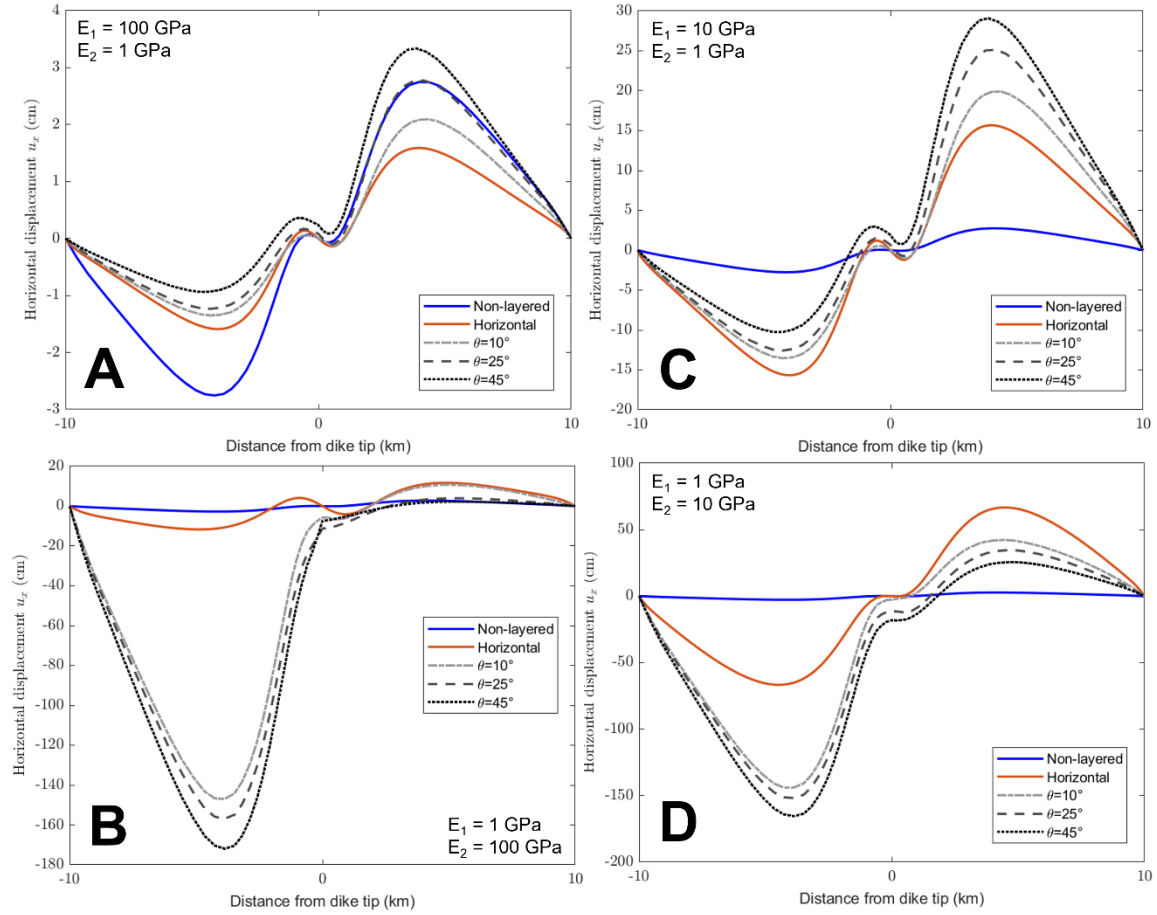


Figure 3: Horizontal ground displacement (u_x) variations relative to the lateral distance from the dike tip for each layer inclination and stiffness contrasts tested.

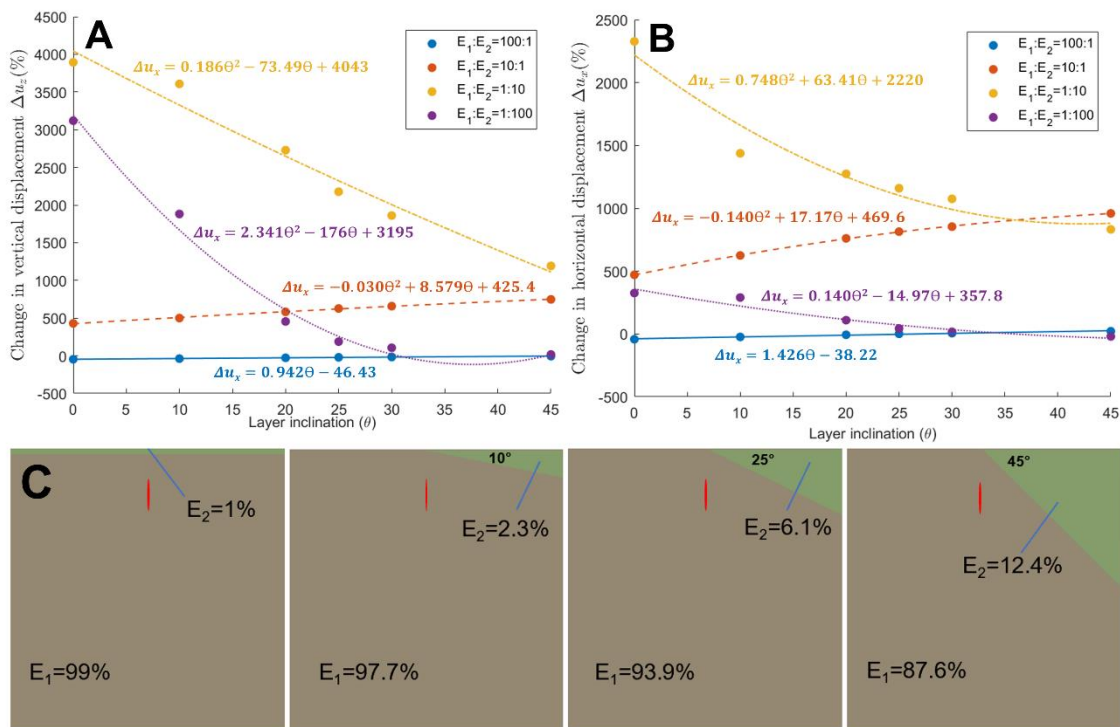


Figure 4: A) and B): Changes in the vertical (Δu_z) and horizontal displacement (Δu_x) in percentages with respect to the non-layered model for each layer inclination (θ) and stiffness ratio tested ($E_1:E_2$). Model fits for each data set are shown allowing comparison between θ and Δu_z or Δu_x . Each individual model fit presents $R^2 > 0.95$. C) Diagrams showing the area ratio in percentages between the modeled crustal segments for different angles of inclination.